Journal of Organometallic Chemistry 694 (2009) 1912–1917

Contents lists available at ScienceDirect

Journal of Organometallic Chemistry

journal homepage: www.elsevier.com/locate/jorganchem

Methyl–oxygen bond cleavage in hemilabile phosphine–ether ligand of ruthenium(II) complexes

Sodio C.N. Hsu [a,*], Shih-Chieh Hu [a], Zih-Shing Wu [a], Michael Y. Chiang [b], Min-Yuan Hung [c]

[a] Department of Medicinal and Applied Chemistry, and Center of Excellence for Environmental Medicine, Kaohsiung Medical University, No. 100, Tzyou 1st Road, Kaohsiung 807, Taiwan
[b] Department of Chemistry, National Sun Yat-Sen University, Kaohsiung 804, Taiwan
[c] Center for Resources, Research and Development, Kaohsiung Medical University, Kaohsiung 807, Taiwan

ARTICLE INFO

Article history:
Received 13 October 2008
Received in revised form 16 January 2009
Accepted 20 January 2009
Available online 24 January 2009

Keywords:
Ruthenium
Phosphine ligands
methyl–oxygen bond cleavage
Dealkylation

ABSTRACT

The preparation and characterization are described for four ruthenium(II) complexes containing hemilabile phosphine–ether ligand *o*-(diphenylphosphino)anisole ($Ph_2PC_6H_4OMe$-*o*) and/or bidentate ligand diphenylphosphino-phenolate ($[Ph_2PC_6H_4O\text{-}o]^-$) $Ru(RCN)_2(\kappa^2\text{-}Ph_2PC_6H_4O\text{-}o)_2$ (**1a**: R = Me; **1b**: R = Et) and $[Ru(RCN)_2(\kappa^2\text{-}Ph_2PC_6H_4O\text{-}o)(\kappa^2\text{-}Ph_2PC_6H_4OMe\text{-}o)](PF_6)$ (**2a**: R = Me; **2b**: R = Et). The ruthenium(II) phosphine–ether complexes undergo mild methyl–oxygen bond cleavage. Two different kinds reaction mechanism are proposed to describe the methyl–oxygen bond cleavage, one involving attack of anionic nucleophiles and another involving the phosphine. The new reactions define novel routes to phosphine–phenolate complexes. The structures of complexes **1a**, **1b** and **2a** were confirmed by X-ray crystallography.

1. Introduction

The insertion of transition-metal atoms into a carbon–oxygen bond is proposed as key steps in the hydrodeoxygenation (HDO) of crude oil and may lead to the design of novel catalytic reactions [1]. The C–O bond cleavage reactions by transition-metal complexes that involve either strained systems or relatively weak C–O bonds, or systems driven by aromatization, are well known [2–9]. For example, C–O bond cleavage of strained cyclic ethers by transition-metals has been applied to catalysis of isomerization to carbonyl compounds, coupling to form esters, and carbonylation to lactones [2,6]. On the other hand, transition-metal complexes contain monoanionic oxygen donor ligands, especially phosphanylphenoxides, are currently receiving considerable attention largely because of their potential use as homogeneous catalyst precursors for polymerization of terminal olefins and ring-opening polymerization of heterocyclic molecules [10–15].

The hemilabile phosphine–ether ligand and its Ru(II) complexes also have received much attention due to their wide-range of utility in homogeneous catalysis [16–18]. Studies of the coordination chemistry of the Ru(II) complexes in particular containing hemilabile phosphine–ether ligands are useful in understanding the catalytic activity of this class of compounds. These phosphine–ether ligands are usually dealkylated when coordinated to transition-metal center to form σ-bonded aryloxide complexes [16,19,20]. Such ligand-assisted dealkylations proceed via nucleophilic attack by the free ligand's phosphorus to produce the stable alkylphosphonium salt, which drives the reaction [20]. Another dealkylation pathway was suggested by the elimination of CH_3Cl in the transition-metal halide complexes [16]. The reactivity of $RuCl_2(\kappa^2\text{-}Ph_2PC_6H_4OMe\text{-}o)_2$ ($Ph_2PC_6H_4OMe$-*o* = *o*-(diphenylphosphino)anisole) has been reported with CO and isocyanide to give mono and di-adducts, which do not perform dealkylation process [21,22]. Herein, we set out to investigate the occurrence of ligand-assisted dealkylation in a $RuCl_2(\kappa^2\text{-}Ph_2PC_6H_4OMe\text{-}o)_2$ complex.

2. Results and discussion

2.1. Ether dealkylation reactions

Thermolysis of $RuCl_2(\kappa^2\text{-}Ph_2PC_6H_4OMe\text{-}o)_2$ in MeCN solvent results in dealkylation of the ether ligands. From this simple procedure we obtained an excellent yield of the neutral compound $Ru(MeCN)_2(\kappa^2\text{-}Ph_2PC_6H_4O\text{-}o)_2$ (**1a**) ($[Ph_2PC_6H_4O\text{-}o]^- = o$-(diphenylphosphino)phenolate)). On the other hand, heating MeCN solution of $RuCl_2(\kappa^2\text{-}Ph_2PC_6H_4OMe\text{-}o)_2$ in the presence of KPF_6 resulted in clean monodemethylation to give the yellow complex $[Ru(MeCN)_2(\kappa^2\text{-}Ph_2PC_6H_4O\text{-}o)(\kappa^2\text{-}Ph_2PC_6H_4OMe\text{-}o)]PF_6$ (**2a**), together with **1a** and a small amounts of phosphonium ion $[Me(Ph_2PC_6H_4OMe\text{-}o)]^+$ (Scheme 1).

* Corresponding author. Tel.: +886 7 3121101; fax: +886 7 3125339.
E-mail address: sodiohsu@kmu.edu.tw (S.C.N. Hsu).

0022-328X/$ - see front matter © 2009 Elsevier B.V. All rights reserved.
doi:10.1016/j.jorganchem.2009.01.032

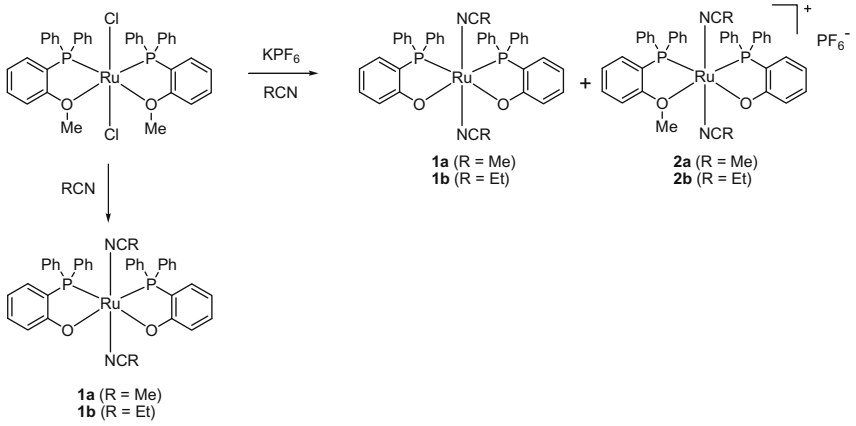

Scheme 1.

Compound **1a** and **2a** both contain two coordinated MeCN ligands which can be confirmed by ^{1}H NMR, ^{13}C{^{1}H}NMR and IR spectroscopy. Additionally each compound gave well-resolved ESI-mass spectra with molecular ions. The ^{1}H NMR spectrum of **1a** shows a singlet at δ 2.08 assigned to the coordinated MeCN. Similarly, a signal for coordinated MeCN is also present in the ^{1}H NMR spectrum of **2a**, in addition a singlet at δ 4.60 assigned to the methoxy group. The ^{13}C{^{1}H}NMR spectrum of **1a** also shows a methyl signal at δ 2.96 and a nitrile signal at δ 122.22, which were assigned to the coordinated MeCN. To compare with **1a**, the ^{13}C{^{1}H}NMR spectrum of **2a** has an extra signal at δ 61.23, which is assigned to methoxy group of undealkylation phosphine–ether ligand. The IR spectrum of **1a** and **2a** both exhibit a weak ν_{CN} band at 2216 and 2260 cm^{-1} assigned to coordinated MeCN, respectively. The ^{31}P{^{1}H} NMR spectrum of **1a** appears only one peak at δ 60.32. The ^{31}P{^{1}H} NMR spectrum of **2a** features two sets of doublet resonances at δ 55.3 and 64.4 in a 1:1 intensity ratio, which may due to different phosphorus environment.

Analogous reactions occurred when the thermolysis of $RuCl_2(\kappa^2\text{-}Ph_2PC_6H_4OMe\text{-}o)_2$ was conducted in EtCN solution, giving $Ru(EtCN)_2(\kappa^2\text{-}Ph_2PC_6H_4O\text{-}o)_2$ (**1b**) and, using KPF_6, $[Ru(EtCN)_2(\kappa^2\text{-}Ph_2PC_6H_4O\text{-}o)(\kappa^2\text{-}Ph_2PC_6H_4OMe\text{-}o)](PF_6)$ (**2b**). Again in the later case, the side products $[Me(Ph_2PC_6H_4OMe\text{-}o)]^+$ was obtained, establishing that the source of the methyl group was the ether, not the solvent. When excess KPF_6 (30 equiv.) was applied in the thermolysis reaction of $RuCl_2(\kappa^2\text{-}Ph_2PC_6H_4OMe\text{-}o)_2$, the amount of CH_3Cl decrease, and the amount of side product phosphonium salt increase (Table 1). A possible explanation may be that the potassium salt (KPF_6) will inhibit the elimination of CH_3Cl to form the potassium chloride during the thermolysis process.

Table 1
Summarized results of reactions of $RuCl_2(\kappa^2\text{-}Ph_2PC_6H_4OMe\text{-}o)_2$ with KPF_6 as determined from experimental separation[a] and ^{1}H NMR spectra[b].

	[a]**1a**	[a]**1b**	[b]CH_3Cl	[b]$[Me(POMe)]^+$
Without KPF_6	88%	–	88%	–
With 2 equiv. KPF_6	67%	20%	66%	6%
With 30 equiv. KPF_6	38%	30%	40%	18%

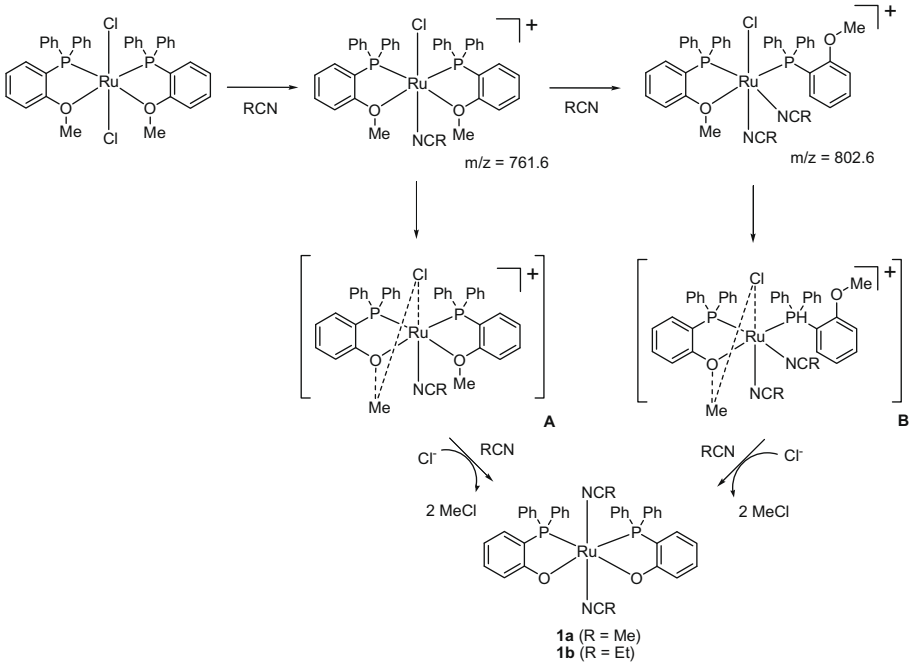

Scheme 2. Proposed reaction pathway for elimination of CH_3Cl without KPF_6.

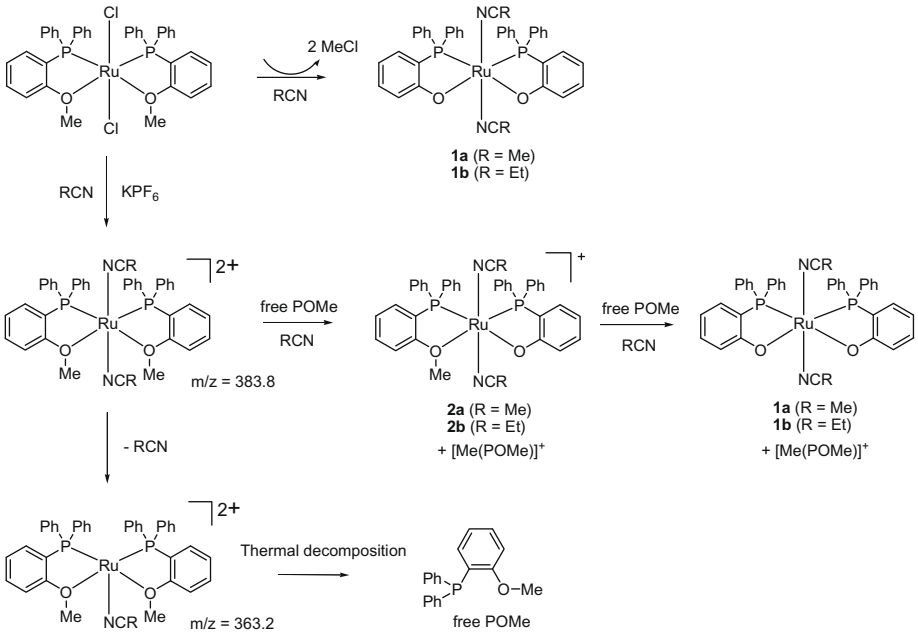

Scheme 3. Probably reaction pathway for the demethylation process in presence of KPF_6.

2.2. In situ studies of the dealkylation

In attempts to examine the possible routes for the formation of demethylation reactions, the thermolysis of $RuCl_2(\kappa^2\text{-}Ph_2PC_6H_4OMe\text{-}o)_2$ was carried out in a sealed NMR tube. Over the course of hours at 80 °C, the ^1H NMR spectra showed the formation of **1a** accompanied the elimination of two molecules of CH_3Cl (δ 3.05, Fig. S2). Related changes were also observed in $^{31}P\{^1H\}$ NMR spectra: the resonance for $RuCl_2(\kappa^2\text{-}Ph_2PC_6H_4OMe\text{-}o)_2$ decreased followed by an increase of the resonance at δ 60.32 for **1a** (Fig. S3).

Different results were obtained when the thermolysis of $RuCl_2(\kappa^2\text{-}Ph_2PC_6H_4OMe\text{-}o)_2$ was conducted in presence of KPF_6. ^1H NMR spectra of showed the formation of **1a**, **2a**, and small amounts of CH_3Cl with a new doublet at δ 2.75, which is assigned to the formation of a phosphonium ion $[Me(Ph_2PC_6H_4OMe\text{-}o)]^+$ (Fig. S4). The $^{31}P\{^1H\}$ NMR spectra data is also consistent with ^1H NMR results (Fig. S5). The reaction of pure **1a**, MeCl (1 atm), and KPF_6 in CD_3CN also carry out in a sealed NMR J-Young tube, which do not give complex **2a** (no reaction occur). On the other hand, the pure **2a** reacts with the free POMe ligand do give **1a**, that was proved by ^{31}P NMR monitoring experiment (Fig. S6). This result appears the additional POMe ligand will assist the O-dealkylation on the ruthenium(II) phosphine–ether complexes.

The thermolysis reaction in MeCN solution of $RuCl_2(\kappa^2\text{-}Ph_2PC_6H_4OMe\text{-}o)_2$ was also examined by ESI-MS, which revealed the formation of some important intermediates prior to dealkylation. The initial ESI-MS experiment of thermolysis MeCN solution of $RuCl_2(\kappa^2\text{-}Ph_2PC_6H_4OMe\text{-}o)_2$ without KPF_6 give the dechlorinate intermediate $[RuCl(\kappa^2\text{-}Ph_2PC_6H_4OMe\text{-}o)_2(NCMe)]^+$ (m/z 761.6) and $[RuCl(\kappa^1\text{-}Ph_2PC_6H_4OMe\text{-}o)(\kappa^2\text{-}Ph_2PC_6H_4OMe\text{-}o)(NCMe)_2]^+$ (m/z 802.6) (Fig. S7). According to the NMR data and ESI-MS

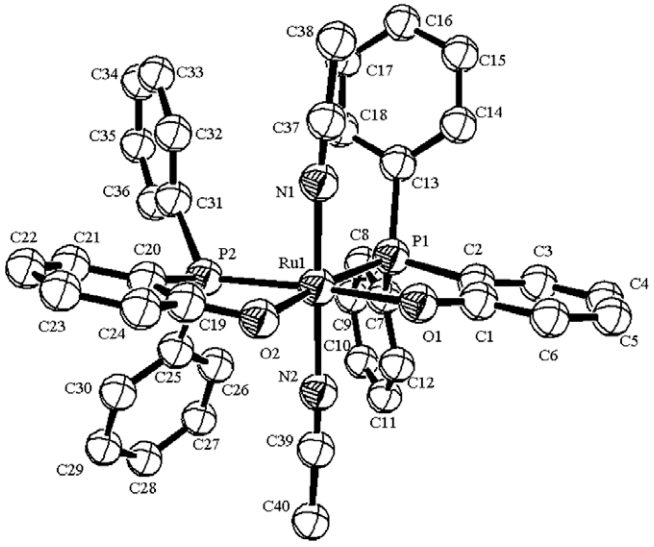

Fig. 1. Molecular structure of $Ru(MeCN)_2(\kappa^2\text{-}Ph_2PC_6H_4O\text{-}o)_2$ (**1a**) with thermal ellipsoids drawn at the 50% level.

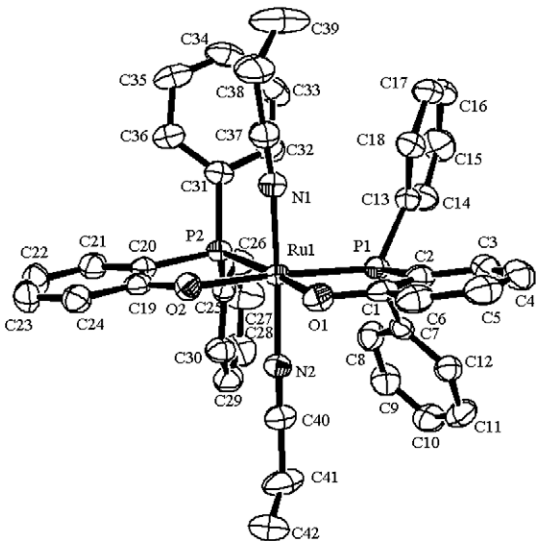

Fig. 2. Molecular structure of $Ru(EtCN)_2(\kappa^2\text{-}Ph_2PC_6H_4O\text{-}o)_2$ (**1b**) with thermal ellipsoids drawn at the 50% level.

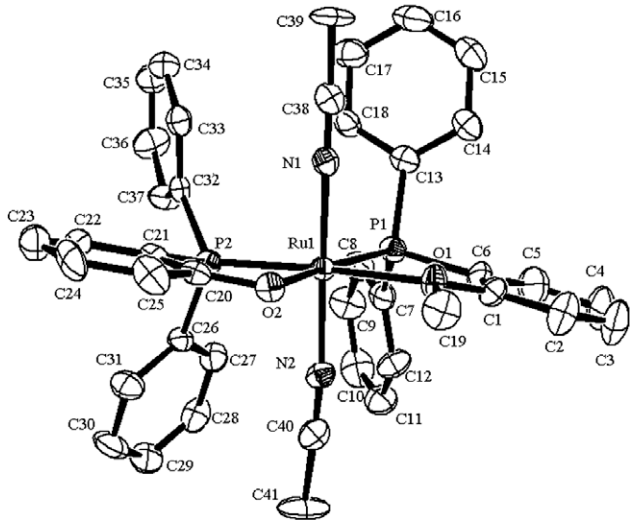

Fig. 3. Molecular structure of the anion $[Ru(MeCN)_2(\kappa^2\text{-}Ph_2PC_6H_4O\text{-}o)(\kappa^2\text{-}Ph_2PC_6H_4OMe\text{-}o)]^+$ (**2a**) with thermal ellipsoids drawn at the 50% level.

Table 2
Selected bond distances (Å) and angeles (deg) for $Ru(CH_3CN)_2(\kappa^2\text{-}Ph_2PC_6H_4O\text{-}o)_2$ (**1a**), $Ru(EtCN)_2(\kappa^2\text{-}Ph_2PC_6H_4O\text{-}o)_2$ (**1b**) and $[Ru(MeCN)_2(\kappa^2\text{-}Ph_2PC_6H_4O\text{-}o)(\kappa^2\text{-}Ph_2PC_6H_4OMe\text{-}o)]PF_6$ (**2a**).

	1a	1b	2a
Ru–O	2.116(2)	2.119(2)	2.105(4)
	2.132(2)	2.125(2)	
Ru–OMe			2.241(4)
Ru–NCMe	2.003(3)	2.005(3)	2.004(5)
	2.013(3)	2.014(3)	2.008(5)
Ru–PO	2.2663(9)	2.2769(8)	2.255(17)
	2.2734(10)	2.2660(9)	
Ru–POMe			2.2800(8)
N–CMe	1.135(5)	1.141(4)	1.150(7)
	1.141(5)	1.136(5)	1.154(7)
P–Ru–P	107.47(4)	107.96(3)	107.22(6)
O–Ru–O	86.86(10)	86.00(8)	89.21(15)
P–Ru–O	82.85(7)	82.99(7)	83.30(12)
	82.84(7)	83.06(6)	
P–Ru–OMe			80.31(11)

results, the proposed reaction pathway of elimination of CH_3Cl is depicted in Scheme 2. The elimination of CH_3Cl may be via a four-centered intermediate or transition state **A** and **B**. Similar reaction pathway has been proposed [16]. On the other hand, the addition of KPF_6 to a MeCN solution of $RuCl_2(\kappa^2\text{-}Ph_2PC_6H_4\text{-}OMe\text{-}o)_2$ was also found to rapidly give the monochloride cations $[RuCl(\kappa^2\text{-}Ph_2PC_6H_4OMe\text{-}o)_2(NCMe)]^+$ (m/z 761.6) and $[RuCl(\kappa^1\text{-}Ph_2PC_6H_4OMe\text{-}o)(\kappa^2\text{-}Ph_2PC_6H_4OMe\text{-}o)(NCMe)_2]^+$ (m/z 802.6) in addition the momo-dealkylation product **2a** (m/z 752.8) present as major species. Interestingly, the dication intermediates $[Ru(\kappa^2\text{-}Ph_2PC_6H_4OMe\text{-}o)_2(NCMe)_2]^{2+}$ (m/z 383.8) and $[Ru(\kappa^2\text{-}Ph_2PC_6H_4OMe\text{-}o)_2(NCMe)]^{2+}$ (m/z 363.2) were only found in the presence of KPF_6 ESI-MS experiment. These initial ESI-mass experiments, which exhibited the corresponding molecular peaks at m/z 761.6, 802.6 and the dication interimediates peaks (m/z 383.8 and 363.2), provided critical data and confirmation of the reaction intermediates. These results indicate the potassium cation may play an important role in the formation of monodemethylation product **2a**.

The presence of the phosphonium ion in reaction products implies that the side reaction comes from the nucleophilic attack of the free phosphine ligand on the carbon of the Ru-bound methoxy group. Similar ligand-assisted *O*-dealkylation are observed for the Ru(II) complexes containing hemilabile phosphine–ether ligand [20,23]. However, the pathway of ligand-assisted *O*-dealkylation still remains unclearly. According to the initial ESI-mass experiment and sealed NMR experiment results, we proposed probably reaction pathway for the demethylation process in presence of KPF_6 (Scheme 3). The initial reaction is chloride dissociation to form the dication intermediates $[Ru(\kappa^2\text{-}Ph_2PC_6H_4OMe\text{-}o)_2(NCMe)_2]^{2+}$ (m/z 383.8) and $[Ru(\kappa^2\text{-}Ph_2PC_6H_4OMe\text{-}o)_2(NCMe)]^{2+}$ (m/z 363.2), which were proved by the initial ESI-mass experiment. The following thermal decomposition of $[Ru(\kappa^2\text{-}Ph_2PC_6H_4OMe\text{-}o)_2\text{-}(NCMe)]^{2+}$ may result in free phosphine ligand for the phosphonium ion formation. There are several probably pathway list in Scheme 3 to explain the final thermolysis result in presence of KPF_6. The driving force of these pathways could come from the side products formation of KCl, CH_3Cl and phosphonium ion $[Me(Ph_2P\text{-}C_6H_4OMe\text{-}o)]^+$. The formation of the phosphonium ion implies that the side reaction arise from nucleophilic attack of the free phosphine on the carbon of the Ru-bound methoxy group. This pathway is predominant when the reaction was conducted in the presence of KPF_6. The potassium salt (KPF_6) may also inhibit the elimination of CH_3Cl, because of the formation of potassium chloride during the thermolysis process.

2.3. Crystallographic characterization of phosphinephenolates

The stereochemistry of **1a**, **1b** and **2a** were determined by single crystal X-ray diffraction analysis (Figs. 1–3; Table 2). The geometry of these complexes is distorted octahedral. All nitrile ligands of **1a**, **1b** and **2a** are nearly symmetrically in mutually *trans* position. The Ru–P bond distances are near 2.27 Å, somewhat longer than those in the starting material $RuCl_2(\kappa^2\text{-}Ph_2PC_6H_4OMe\text{-}o)_2$ (2.217 Å) [21]. This effect arises from greater *trans* influence of the phenoxide versus the more weakly donating ether ligands trans to the phosphine. The P–Ru–P angles are approximately 107°, presumably minimizing repulsive interactions between the phenyl groups. The O–Ru–O angles are 20° more acute in **1a**, **1b**, and **2a**. The $Ph_2PC_6H_4O\text{-}o$ ligand functions has a chelate bite angles P–Ru–O of 83.30°, slightly larger than the P–Ru–OMe of 80.31° in **2a**. Most significantly, the Ru–O (phenoxide) distances of 2.116 Å and 2.132 Å in **1a**, 2.119 Å and 2.125 Å in **1b**, and 2.105 Å in **2a** are much shorter than Ru–O (ether) bond distance of 2.241 Å in **2a** and their starting material $RuCl_2(\kappa^2\text{-}Ph_2PC_6H_4OMe\text{-}o)_2$ (2.229 and 2.257 Å) [21]. In the mixed ether-phenoxide complex **2a**, Ru–OMe bond distance of 2.241 Å is much longer than the sum of the covalent radii (1.99 Å), suggesting that the oxygen atom of ether group is only weakly coordinated [24]. In fact, complex **2a** contains both Ru–O and Ru–OMe types bonding mode in a complex that gives a good example to compare the weak metal–ether bonds versus strong metal–phenoxide bonds.

3. Conclusions

Four ruthenium(II) complexes containing hemilabile phosphine–ether ligand *o*-(diphenylphosphino)anisole ($Ph_2PC_6H_4\text{-}OMe\text{-}o$) and/or bidentate ligand diphenylphosphino–phenolate have been synthesized and characterized in order to examine the possible routes for the methyl–oxygen bond cleavage. Two different kinds reaction mechanism are proposed to describe the methyl–oxygen bond cleavage, one involving the elimination of CH_3Cl molecule and another involving the formation of the phosphonium ion. It is first time to observe the elimination of CH_3Cl and the formation of the phosphonium ion in a reaction, which may provide us a good example to study the condition of ligand-assisted *O*-dealkylation of transition-metal complexes.

4. Experimental

All manipulations were carried out under an atmosphere of purified dinitrogen with standard Schlenk techniques. Chemical reagents were purchased from Aldrich Chemical Company Ltd., Lancaster Chemicals Ltd., or Fluka Ltd. All the reagents were used without further purification, apart from all solvents that were dried over Na (Et_2O, hexane, THF) or CaH_2 (CH_2Cl_2, CH_3CN) or dried via filtration through activated alumina then thoroughly degassed before use. $RuCl_2(\kappa^2\text{-}Ph_2PC_6H_4OMe\text{-}o)_2$ were prepared according to literature procedures [21]. IR spectra were recorded on a Perkin–Elmer System 2000 FTIR spectrometer. ^1H and ^{31}P NMR spectra were acquired on a Varian Gemini-500 proton/Carbon FT NMR spectrometer at 500 and 202.4 MHz, respectively. ESI-MS were collected on a Quattro quadrupole–hexapole–quadrapole (QHQ) mass spectrometer. Elemental analyses were performed by by the National Science Council Regional Instrumentation Center at National Chen-Kung University, Tainan, Taiwan.

4.1. Thermolysis of $RuCl_2(\kappa^2\text{-}Ph_2PC_6H_4OMe\text{-}o)_2$ in MeCN

A solution of 360 mg (0.48 mmol) of $RuCl_2(\kappa^2\text{-}Ph_2PC_6H_4\text{-}OMe\text{-}o)_2$ was refluxed in 30 mL of CH_3CN for 4 h. The color of the reaction mixture changed from red to yellow with yellow suspended solid. The yellow solid was collected by filtration to give a yellow product $Ru(MeCN)_2(\kappa^2\text{-}Ph_2PC_6H_4O\text{-}o)_2$ (**1a**). Yield: 309 mg (88%). IR (KBr, cm^{-1}): ν_{CN} = 2216(w). ^1H NMR (DMSO-d^6): δ *2.08 (s,* 6H, CH_3CN), 4.60 (s, 3H, -OCH_3), 6.95–7.90 (m, 28H, Ph). $^{13}C\{^1H\}$NMR (DMSO-d^6): δ 2.96 (*C*H_3CN), 122.22 (CH$_3$*C*N), 112.41–179.66 (Ph). $^{31}P\{^1H\}$NMR (CD_2Cl_2): δ 60.40(s). ESI-MS (*m*/*z*): 739.4 ([M+H]$^+$), 698.3 ([M−(CH$_3$CN)+H]$^+$), 657.2 ([M−(CH$_3$CN)$_2$+H]$^+$). Anal. Calc. for $C_{40}H_{34}N_2O_2P_2RuCH_2Cl_2$: C, 59.86; H, 4.41; N, 3.41. Found: C, 59.78; H, 4.49; N, 3.46%.

4.2. Thermolysis of $RuCl_2(\kappa^2\text{-}Ph_2PC_6H_4OMe\text{-}o)_2$ with KPF_6 in MeCN

A solution of 360 mg (0.48 mmol) of $RuCl_2(\kappa^2\text{-}Ph_2PC_6H_4\text{-}OMe\text{-}o)_2$ and 176 mg (0.96 mmol) of KPF_6 was refluxed in 30 mL of CH_3CN for 18 h. The color of the reaction mixture changed from red to yellow with yellow and white suspended solid. The yellow filtrate collected by filtration and reduced ca. 3 mL under vacuum, followed by the addition of 50 mL of ether to give yellow microcrystals of $[Ru(CH_3CN)_2(\kappa^2\text{-}Ph_2PC_6H_4O\text{-}o)(\kappa^2\text{-}Ph_2PC_6H_4OMe\text{-}o)](PF_6)$ (**2a**). Yield: 85 mg (20%). The yellow filtration solid was extracted into 10 mL of CH_2Cl_2 followed by addition of 100 mL of ether to give a yellow product $Ru(MeCN)_2(\kappa^2\text{-}Ph_2PC_6H_4O\text{-}o)_2$ (**1a**). Yield: 235 mg (67%). *trans*-$[Ru(CH_3CN)_2(\kappa^2\text{-}Ph_2PC_6H_4O\text{-}o)(\kappa^2\text{-}Ph_2PC_6H_4OMe\text{-}o)](PF_6)$ (**2a**): IR (KBr, cm^{-1}): ν_{CN} = 2260 (w). ^1H NMR (DMSO-d^6): δ *2.08 (s,* 6H, CH_3CN), 4.60 (s, 3H, -OCH_3), 6.95–7.90 (m, 28H, Ph). $^{13}C\{^1H\}$NMR (DMSO-d^6): δ 9.55 (*C*H$_3$CN), 61.23 (-OCH$_3$), 125.43 (CH$_3$*C*N), 112.62–179.02 (Ph). $^{31}P\{^1H\}$NMR (DMSO-d^6): δ 64.45 (d, J_{PP} = 60 Hz), 55.32 (d, J_{PP} = 60 Hz). ESI-MS (*m*/*z*): 753.2 (M$^+$). Anal. Calc. for $C_{41}H_{37}F_6N_2O_2P_3Ru$: C, 54.85; H, 4.15; N, 3.12. Found: C, 54.96; H, 4.19; N, 3.25%.

4.3. Thermolysis of $RuCl_2(\kappa^2\text{-}Ph_2PC_6H_4OMe\text{-}o)_2$ in EtCN

A solution of 360 mg (0.48 mmol) of $RuCl_2(\kappa^2\text{-}Ph_2PC_6H_4\text{-}OMe\text{-}o)_2$ was refluxed in 30 mL of EtCN for 4 h. The color of the reaction mixture changed from red to yellow with yellow suspended solid. The yellow solid was collected by filtration to give a yellow product $Ru(EtCN)_2(\kappa^2\text{-}Ph_2PC_6H_4O\text{-}o)_2$ (**1b**). Yield: 308 mg (84%). ^1H NMR (CD_2Cl_2): δ 0.47 (t, 6H, CH_3CH$_2$CN), 1.85 (q, 4H, CH$_3$CH_2CN), 6.43–7.31 (m, 28H, Ph). $^{13}C\{^1H\}$NMR (CD_2Cl_2): δ 9.55 (*C*H$_3$CH$_2$CN), 12.94 (CH$_3$CH$_2$CN), 125.12 (CH$_3$CH$_2$*C*N), 112.62–179.02 (Ph) $^{31}P\{^1H\}$NMR (CD_2Cl_2): δ 59.24(s). ESI-Mass (*m*/*z*): 767.6 ([M+H]$^+$), 711.19 ([M−EtCN+H]$^+$). Anal. Calc. for $C_{42}H_{38}N_2O_2$-P_2Ru: C, 65.87; H, 5.00; N3.66. Found: C, 65.83; H, 5.11; N, 3.58%.

4.4. Thermolysis of $RuCl_2(\kappa^2\text{-}Ph_2PC_6H_4OMe\text{-}o)_2$ with KPF_6 in EtCN

A solution of 360 mg (0.48 mmol) of $RuCl_2(\eta^2\text{-}Ph_2PC_6H_4OMe\text{-}o)_2$ and 176 mg (0.96 mmol) of KPF_6 was refluxed in 30 mL of EtCN for 18 h. The color of the reaction mixture changed from red to yellow with yellow and white suspended solid. The yellow filtrate collected by filtration and reduced ca. 3 mL under vacuum, followed by the addition of 50 mL of ether to give yellow microcrystals of $[Ru(EtCN)_2(\kappa^2\text{-}Ph_2PC_6H_4O\text{-}o)(\kappa^2\text{-}Ph_2PC_6H_4OMe\text{-}o)](PF_6)$ (**2b**). Yield: 133 mg (30%). The yellow filtration solid was extracted into 10 mL of CH_2Cl_2 followed by addition of 100 mL of ether to give a yellow product $Ru(EtCN)_2(\kappa^2\text{-}Ph_2PC_6H_4O\text{-}o)_2$ (**1b**). Yield: 184 mg (50%). *trans*-$[Ru(EtCN)_2(\kappa^2\text{-}Ph_2PC_6H_4O\text{-}o)(\kappa^2\text{-}Ph_2PC_6H_4OMe\text{-}o)](PF_6)$ (**2b**): ^1H NMR (DMSO-d^6): δ 1.14 (t, 6H, CH_3CH$_2$CN), 2.10 (q, 4H, CH$_3$ CH_2CN), 4.38 (s, 3H, -OCH_3), 6.35–7.42 (m, 28H, Ph). $^{13}C\{^1H\}$NMR

Table 3
Crystallographic data for $Ru(CH_3CN)_2(\kappa^2\text{-}Ph_2PC_6H_4O\text{-}o)_2$ (**1a**), $Ru(EtCN)_2(\kappa^2\text{-}Ph_2PC_6H_4O\text{-}o)_2$ (**1b**) and $[Ru(MeCN)_2(\kappa^2\text{-}Ph_2PC_6H_4O\text{-}o)(\kappa^2\text{-}Ph_2PC_6H_4OMe\text{-}o)]PF_6$ (**2a**).

	1a · $3CH_2Cl_2$	**1b** · CH_3OH	**2a** · CH_3CN
Empirical formula	$C_{43}H_{40}C1_6N_2O_2P_2Ru$	$C_{45}H_{50}N_2O_5P_2Ru$	$C_{43}H_{40}F_6N_3O_2P_3Ru$
Formula weight	992.48	861.88	939.13
T (K)	193(2)	200(2)	293(2)
Crystal system	Triclinic	Monoclinic	Monoclinic
Space group	$P\bar{1}$	$P2_1/c$	$P2_1/c$
a (Å)	9.6937(5)	16.7345(2)	9.863(2)
b (Å)	14.2709(7)	12.9796(2)	22.457(5)
c (Å)	16.5212(8)	19.4951(3)	19.373(4)
α (°)	100.690(3)	90	90
β (°)	100.348(3)	95.2900(10)	101.51(3)
γ (°)	91.795(3)	90	90
V (Å^3)	2204.37(19)	4216.44(10)	4204.8(15)
Z	2	4	4
D_{calc} (g cm^{-3})	1.495	1.358	1.464
μ (mm^{-1})	0.830	0.494	0.138
Reflections measured/independent	27536/9075	36023/7423	51952/7990
Data/restraints/parameters	9075/102/563	7423/0/500	7990/0/509
Goodness-of-fit	1.098	1.192	0.885
R_{int}	0.0463	0.0443	0.1712
R_1 [$I > 2\sigma$] (all data)	0.0439 (0.0755)	0.0419 (0.0579)	0.0519 (0.1382)
R_w [$I > 2\sigma$] (all data)	0.1022 (0.1209)	0.1090 (0.1305)	0.1208 (0.1508)
Maximum peak/hole (e$^-$/Å^3)	0.910/−1.050	0.944/−0.946	0.933/−0.421

(DMSO-d^6): δ 9.55 (CH_3CN), 12.94 (CH_3CH_2CN), 60.45 (-OCH_3), 124.56 (CH_3CH_2CN), 112.62–179.02 (Ph). $^{31}P\{^1H\}$NMR (MeCN-d^3): δ 64.12 (d, J_{PP} = 24.2 Hz), 54.45 (d, J_{PP} = 36 Hz). ESI-Mass (m/z): 781.2 (M^+), 726.2 ([M–EtCN]$^+$). Anal. Calc. for $C_{43}H_{41}F_6N_2O_2P_3Ru$: C, 55.79; H, 4.46; N, 3.03. Found: C, 55.74; H, 4.39; N, 3.15%.

4.5. Preparation of phosphonium salt [Me(POMe)]I

An excess of MeI (0.20 mL, 3.22 mmol) was added to a solution of 2-methoxyphenyldiphenylphosphine (0.20 g, 0.673 mmol) in dry diethyl ether (25 mL) under nitrogen. The mixture immediately became cloudy upon formation of the insoluble phosphonium salt. The mixture was stirred for 5 h then evaporated to dryness to remove excess MeI. The residue was suspended in ether and the white powder collected by filtration, washed with ether and hexanes, and dried under vacuum. Yield: 96%. $^{31}P\{^1H\}$ NMR (MeCN-d^3): δ 21.9 (s). ^1H NMR (MeCN-d^3): δ 2.75 (d, $^2J_{PH}$ = 14.4 Hz, 3H), 3.76 (s, 3H, MeO), 7.23–7.97 (m, 14H, Ph).

4.6. Crystallography

A single crystal suitable for X-ray analysis of complex **1a** was obtained by diffusion of E_2O into CH_2Cl_2 solution. For crystal sample of complexes **1b** was obtained by diffusion of Et_2O into CH_3OH solution. Single crystals suitable for X-ray analysis of complex **2a** were obtained by diffusion of Et_2O into CH_3CN solution. All crystals were mounted on a thin glass fiber by using oil (Paratone-N, Exxon) before being transferred to the diffractometer. Data were collected on a Siemens CCD automated diffractometer or a Bruker Nonius Kappa CCD diffractometer at low temperature. Data processing was performed with the integrated program package SHELXTL [25]. All structures were solved using direct methods and refined using full-matrix least squares on F^2 using the program SHELXL-97 [26]. All hydrogen atoms were fixed in idealized positions with thermal parameters 1.5 times those of the attached carbon atoms. The data were corrected for absorption on the basis of ¾ scans. Specific details for each crystal are given in Table 3.

Acknowledgements

We gratefully acknowledge the financial support of the National Science Council (Taiwan). We thank Mr. Ting-Shen Kuo (National Taiwan Normal University) for solving the X-ray structure of Ru(EtCN)2(κ^2-$Ph_2PC_6H_4O$-o)$_2$(**1b**) and Prof. T.B. Rauchfuss for helpful discussions.

Appendix A. Supplementary material

CCDC 701446, 701447 and 701448 contain the supplementary crystallographic data of compounds **1a**, **1b** and **2a** for this paper. These data can be obtained free of charge from the Cambridge Crystallographic Data Centre via www.ccdc.cam.ac.uk/data_request/cif. Supplementary data associated with this article can be found, in the online version, at doi:10.1016/j.jorganchem.2009.01.032.

References

[1] J.H. Gary, G.E. Handwerk, M.J. Kaiser, Petroleum Refining: Technology and Economics, 5th ed., CRC, New York, 2007.
[2] D. Milstein, Acc. Chem. Res. 17 (1984) 221–226.
[3] K.T. Aye, D. Colpitts, G. Ferguson, R.J. Puddephatt, Organometallics 7 (1988) 1454–1456.
[4] A.A. Zlota, F. Frolow, D. Milstein, J. Am. Chem. Soc. 112 (1990) 6411–6413.
[5] D. Rondon, B. Chaudret, X.D. He, D. Labroue, J. Am. Chem. Soc. 113 (1991) 5671–5676.
[6] K. Khumtaveeporn, H. Alper, Acc. Chem. Res. 28 (1995) 414–422.
[7] S.-Y. Liou, M.E. Van der Boom, Y. Ben-David, L.J.W. Shimon, D. Milstein, J. Am. Chem. Soc. 120 (1998) 6531–6541.
[8] H. Weissman, L.J.W. Shimon, D. Milstein, Organometallics 23 (2004) 3931–3940.
[9] M.E.V.D. Boom, S.-Y. Liou, L.J.W. Shimon, Y. Ben-David, D. Milstein, Inorg. Chem. Acta 357 (2004) 4015–4023.
[10] C.A. Willoughby, J. Ronald, R. Duff, W.M. Davis, S.L. Buchwald, Organometallics 15 (1996) 472–475.
[11] S. Priya, M.S. Balakrishna, J.T. Mague, Chem. Lett. 33 (2004) 308–309.
[12] R.J. Long, V.C. Gibson, A.J.P. White, D.J. Williams, Inorg. Chem. 45 (2006) 511–513.
[13] L.-C. Liang, Y.-N. Chang, H.M. Lee, Inorg. Chem. 46 (2007) 2666–2673.
[14] P. Kuhn, D. Śemeril, D. Matt, M.J. Chetcuti, P. Lutz, Dalton Trans. (2007) 515–528.
[15] R.J. Long, V.C. Gibson, A.J.P. White, Organometallics 27 (2008) 235–245.
[16] Y. Yamamoto, R. Sato, F. Matsuo, C. Sudoh, T. Igoshi, Inorg. Chem. 35 (1996) 2329–2336.
[17] S. Priya, M.S. Balakrishna, J.T. Mague, J. Organomet. Chem. 689 (2004) 3335–3349.
[18] M.A. Moreno, M. Haukka, S. Jääskeläinen, S. Vuoti, J. Pursiainen, T.A. Pakkanen, J. Organomet. Chem. 690 (2005) 3803–3814.
[19] A. Bader, E. Lindner, Coord. Chem. Rev. 108 (1991) 27–110.
[20] C.W. Rogers, B.O. Patrick, S.J. Rettig, M.O. Wolf, J. Chem. Soc., Dalton Trans. (2001) 1278–1283.
[21] J.C. Jeffrey, T.B. Rauchfuss, Inorg. Chem. 18 (1979) 2658–2666.
[22] T.B. Rauchfuss, F.T. Patino, D.M. Roundhill, Inorg. Chem. 14 (1975) 652–656.
[23] Y. Yamamoto, K.-I. Sugawara, T. Aiko, J.-F. Ma, J. Chem. Soc., Dalton Trans. (1999) 4003–4008.
[24] L. Pauling, Nature of the Chemical Bond, 3rd ed., Cornell University Press, Ithaca, NY, 1960.
[25] G.M. Sheldrick, SHELXTL, Bruker AXS Madison, 1998.
[26] G.M. Sheldrick, SHELXL-97, University of Gottingen, Gottingen, 1997.